blood®
Regular Article

MYELOID NEOPLASIA

Mutated *SETBP1* activates transcription of Myc programs to accelerate *CSF3R*-driven myeloproliferative neoplasms

Sarah A. Carratt, Garth L. Kong, Brittany M. Curtiss, Zachary Schonrock, Lauren Maloney, Breanna N. Maniaci, Hunter Z. Blaylock, Adrian Baris, Brian J. Druker, Theodore P. Braun, and Julia E. Maxson

Knight Cancer Institute, Oregon Health & Science University, Portland, OR

KEY POINTS

- **We found that mutated *SETBP1* enhances transcription of *Myc* and Myc target genes to promote aggressive disease biology.**
- **In cell line models and human *SETBP1*-mutated CNL cells, these oncogenic programs can be reversed by LSD1 inhibitors.**

Colony stimulating factor 3 receptor (*CSF3R*) mutations lead to JAK pathway activation and are the molecular hallmark of chronic neutrophilic leukemia (CNL). Approximately half of patients with CNL also have mutations in SET binding protein 1 (*SETBP1*). In this study, we developed models of *SETBP1*-mutated leukemia to understand the role that SETBP1 plays in CNL. *SETBP1* mutations promote self-renewal of *CSF3R*-mutated hematopoietic progenitors in vitro and prevent cells from undergoing terminal differentiation. In vivo, *SETBP1* mutations accelerate leukemia progression, leading to the rapid development of hepatosplenomegaly and granulocytosis. Through transcriptomic and epigenomic profiling, we found that *SETBP1* enhances progenitor-associated programs, most strongly upregulating *Myc* and Myc target genes. This upregulation of *Myc* can be reversed by LSD1 inhibitors. In summary, we found that *SETBP1* mutations promote aggressive hematopoietic cell expansion when expressed with mutated *CSF3R* through the upregulation of Myc-associated gene expression programs.

Introduction

Chronic neutrophilic leukemia (CNL) is a rare myeloproliferative neoplasm characterized by the overproduction of neutrophils. Colony stimulating factor 3 receptor (*CSF3R*) mutations are the molecular hallmark of CNL and lead to ligand-independent receptor dimerization and downstream JAK pathway activation.[1] Historically, treatment options for CNL were limited. The discovery of activating *CSF3R* mutations in CNL led to the identification of JAK inhibitors as a potential targeted therapeutic strategy for these patients. In a clinical trial for patients with CNL and atypical chronic myeloid leukemia, a 54% overall response rate was achieved with the JAK1/2 inhibitor ruxolitinib in those patients who had mutations in *CSF3R*.[2] Although targeting CSF3R signaling with ruxolitinib has shown clinical efficacy, responses have not always been durable. Anecdotally, the small number of long-term responders tends to have less genetic complexity. Treatment of CNL will therefore likely require a multipronged therapeutic approach to improve initial treatment response rates and prevent the development of acquired resistance.

One of the most commonly comutated genes in CNL is SET binding protein 1 (*SETBP1*), which is mutated in approximately half of cases.[2] In myeloid leukemia, *SETBP1* mutations predominantly occur in the β-TrCP degron motif. One of the two most common point mutations, D868N, is used in these studies. *SETBP1* point mutations interfere with the ubiquitination and subsequent degradation of SETBP1, resulting in an accumulation of SETBP1-mutated protein.[3] Mutations in *SETBP1* are often associated with poor prognosis in myeloid malignancies[4]; however, high levels of wild-type (WT) *SETBP1* also drive adverse outcomes in acute myeloid leukemia.[5]

SETBP1 regulates tumor suppressor pathways and modulates transcription.[3,6-8] SETBP1 is a binding partner of SET, a 39-kDa protein that inhibits the tumor suppressor protein phosphatase 2A.[9] SETBP1 has also been implicated as a transcriptional regulator in murine leukemia models, conferring increased self-renewal capacity through enhanced expression of *Hoxa9*, *Hoxa10*, and *Myb* and repression of *Runx1* expression.[6,8,10] In a human embryonic kidney model (Flp-In 293), SETBP1 was shown to recruit the MLL1 transcriptional activator complex and directly upregulate *MECOM* and MECOM target genes.[7] Recently, we found that SETBP1 can modulate disease biology driven by cooccurring mutations.[11] Specifically, in the context of Ras pathway–driven leukemia, mutated SETBP1 can increase MAPK pathway activation.[11] The goal of this study was to understand the context-specific role of *SETBP1* mutations in CNL to enable the development of therapeutic approaches that improve treatment outcomes for these patients.

In this study, we investigated how *SETBP1* modulates *CSF3R*-driven disease biology. In a murine model of *CSF3R*-driven CNL, we found that the addition of a *SETBP1* mutation enhances cellular proliferation and accelerates disease progression. In a cell line expressing mutated *SETBP1*, we found that one of the strongest proliferation-associated signatures is that of MYC target genes. Expression of mutated *SETBP1* both increases

Myc gene expression and activates an MYC E-box luciferase reporter. When we assessed SETBP1-driven histone modulation, we identified a 67% overlap between Myc binding sites and H3K4me3 marks upregulated by SETBP1, indicating an overlap in the promoters that are regulated by Myc and SETBP1. Treatment with lysine-specific demethylase 1 (LSD1) inhibitors decreased *Myc* expression by at least 70% for each of the 3 inhibitors evaluated (GSK2879552, GSK-LSD1, and ORY-1001). LSD1 inhibitors caused synergistic cell death when combined with the JAK inhibitor ruxolitinib. As a mutation that drives robust proliferation in our model systems, *SETBP1* represents a promising candidate for targeted therapeutic development.

Methods

Detailed methods are available in the data supplement.

Murine models

C57BL/6J mice (catalog #000664) and Balb/cJ mice (catalog #000651) were obtained from The Jackson Laboratories. Murine transplantation methods and models derived from mice (colony-forming unit [CFU] assays and cell lines) are described in the data supplement.

Flow cytometry

Cells were stained for Cd11b, GR-1, Ly-6G, and/or propidium iodide and analyzed using a BD FACSAria III and FlowJo (10.7.2) and FSC Express 7 research software.

RNA sequencing

First, doxycycline was withdrawn from the *CSF3R*^{T618I} plus *SETBP1*$^{D868N\text{-dox}}$ cell line by washing the cells with phosphate-buffered saline (PBS) 5 times and then resuspending the cells in triplicate with or without 1 μM of doxycycline. Next, in quadruplicate, the *CSF3R*^{T618I} plus *SETBP1*$^{D868N\text{-dox}}$ cell line was treated with dimethyl sulfoxide (DMSO), 100 nM of ruxolitinib, 100 nM of GSK2879552, 30 nM of ORY-1001, ruxolitinib with GSK2879552, or ruxolitinib with ORY-1001. For both experiments, RNA was extracted from cells at 24 hours posttreatment using the RNeasy Micro Kit (Qiagen). Complementary DNA libraries were constructed using the Takara SmartSeq for Ultra Low Input Kit and sequenced using a HiSeq 2500 Sequencer (Illumina; 100 bp, single read). Raw reads were trimmed with Trimmomatic[12] and aligned with STAR.[13] Bioinformatic analyses were performed using Enrichr,[14,15] gene set enrichment analysis (GSEA),[16,17] and HOMER.[18]

CUT&Tag

Doxycycline was withdrawn from the *CSF3R*^{T618I} plus *SETBP1*$^{D868N\text{-dox}}$ cell line by washing the cells with PBS 5 times and then resuspending the cells in duplicate with or without 1 μM of doxycycline. CUT&Tag methods were performed as previously described[19,20] and as described in the data supplement.

Promoter assay

A pGL2M4-luc reporter plasmid[21] (containing 4 CACGTG binding sites and a canonical E-box) and pRL *Renilla* luciferase control reporter vectors (cytomegalovirus promoter; catalog #E2231; Promega) were transiently transfected into 293T17 cells. Luciferase activity was quantified using the Promega Dual-Luciferase Reporter Assay System (catalog #E1910) with the BioTek Synergy2 plate reader.

Inhibitor screening and synergy analysis

A chemical screen was performed as described previously.[22] Synergy analysis in Figure 7 was performed by plating the *CSF3R*^{T618I} plus *SETBP1*^{D868N} cell line in an 8 × 8 matrix in triplicate with increasing concentrations of each inhibitor. Viability was assessed at 72 hours using a tetrazolamine-based (MTS) assay, and synergy was calculated with SynergyFinder.[23] Synergy in supplemental Figure 8 was calculated by Bliss additivity analysis.[24]

qPCR

The *SETBP1*$^{D868N\text{-dox}}$ cell line was treated with GSK2879552 (1000 nM), GSK-LSD1 (100 nM), or JQ1 (200 nM) for 48 hours, and quantitative polymerase chain reaction (qPCR) was performed for *Myc*. The *CSF3R*^{T618I} plus *SETBP1*^{D868N} cell line was treated with 1 of 3 LSD1 inhibitors at 100 nM (GSK2879552) or 30 nM (GSK-LSD1 or ORY-1001) for 48 hours. Key RNA sequencing (RNA-seq) findings were validated by qPCR.

CITE-seq

Live CD34^{+} progenitor cells were isolated from a CNL bone marrow sample with *CSF3R*^{T618I} and *SETBP1*^{G870S} mutations and expanded in culture for 7 days. A total of 300 000 cells were then treated with 100 nM of either ORY-1001 or DMSO for 24 hours. After treatment, single-cell RNA-seq with barcoded antibody labeling (CITE-seq) was performed, as detailed in the data supplement.

Data presentation

All graphs were made using either ggPlot2, GSEA, or GraphPad Prism; figures were assembled in Adobe Illustrator and Affinity Designer. Data are presented as mean ± standard error of the mean.

Results

One of the primary goals of this study was to understand how the presence of an *SETBP1* mutation alters *CSF3R*-driven phenotypes in both murine and in vitro models. To understand how mutated *SETBP1* modulates the phenotypes associated with a *CSF3R* point mutation (T618I), we first performed a murine hematopoietic CFU assay. In this assay, primary mouse bone marrow cells were transduced with retroviral vectors to express mutations of interest, and 5000 sorted cells per condition were plated in cytokine-free methylcellulose. Interestingly, although *CSF3R*^{T618I} expressed alongside an empty vector control led to the formation of large dispersed colonies, neither *SETBP1*^{WT} nor *SETBP1*^{D868N} with empty vector stimulated any colony formation in the absence of cytokines (Figure 1A). When combined with *CSF3R*^{T618I}, overexpression of *SETBP1* (either *SETBP1*^{WT} or *SETBP1*^{D868N}) significantly augmented colony formation, and the colonies had large dense centers (Figure 1A-B). This augmentation by *SETBP1*^{WT} driven by a strong promoter is consistent with the known mechanism of *SETBP1*^{D868N} in driving oncogenesis through protein overexpression. Cytospins prepared from individual colonies showed that they were primarily composed of myeloid cells (Figure 1C).

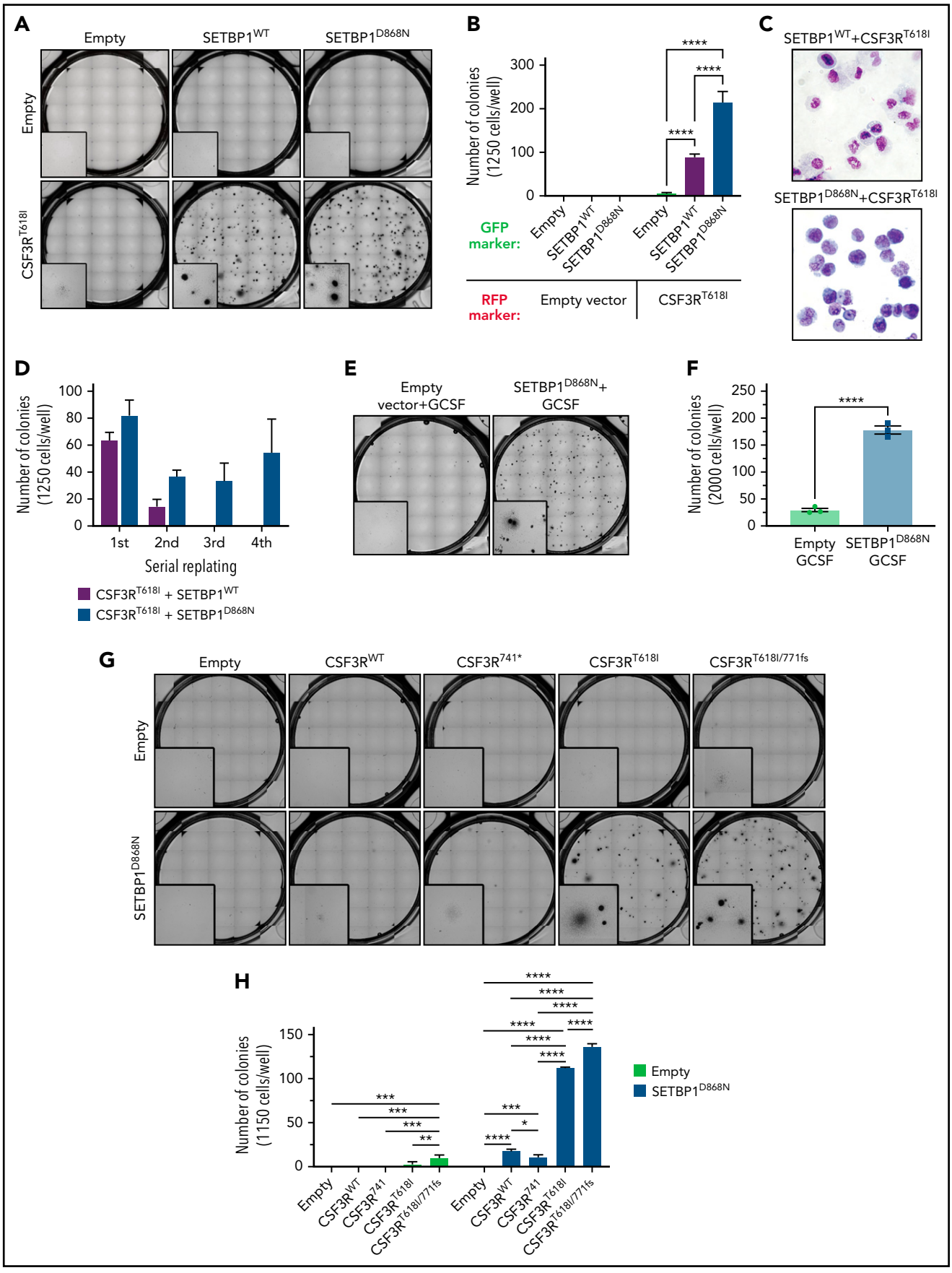

Figure 1.

To determine whether expression of both oncogenes conferred replating potential, colonies were harvested and washed with PBS, and ~10 000 cells were resuspended in fresh cytokine-free methylcellulose. Both *CSF3R*^{T618I} plus *SETBP1*^{WT} and *CSF3R*^{T618I} plus *SETBP1*^{D868N} expression in cells conferred replating potential out to at least the fourth passage in CFU assay (Figure 1D). We previously reported that *SETBP1*^{D868N} enhanced *NRAS*^{G12D} CFU formation and replating potential through the upregulation of MAPK signaling.[11] MAPK activation was not decreased when the SET binding domain[9] (ΔSET) was deleted from SETBP1. To assess the role of the SET binding domain in the synergy between *CSF3R*^{T618I} and *SETBP1*^{D868N}, we overexpressed *SETBP1*$^{\Delta SET}$ with *CSF3R*^{T618I} and performed a CFU assay (supplemental Figure 1A). Deletion of the SET binding domain from *SETBP1*^{D868N} did not decrease the number of CFUs formed with *CSF3R*^{T618I} (supplemental Figure 1B). Adding a premature stop codon to *SETBP1*^{D868N} at either the start of the SET binding domain or the start of the second AT hook resulted in a loss of synergy with *CSF3R*^{T618I} (supplemental Figure 1C).

To determine if *SETBP1*^{D868N} can augment proliferation driven by activation of endogenous CSF3R, cells expressing either *SETBP1*^{D868N} or an empty vector were plated in methylcellulose with 100 nM of granulocyte colony-stimulating factor (GCSF), the ligand for CSF3R. In this assay, GCSF-driven colony formation increased by a factor of 6 when *SETBP1*^{D868N} was expressed (Figure 1E-F). Because of the synergy between *SETBP1*^{D868N} and GCSF, we wondered if there would be synergy between *SETBP1*^{D868N} and either *CSF3R*^{WT} or other *CSF3R* mutations known to affect signaling output.[1,22-25] In CFU assay (Figure 1G-H), the *CSF3R* compound mutation (*CSF3R*$^{T618I/771fs}$) had significantly more colonies than *CSF3R*^{T618I}, whether it was expressed with empty vector or *SETBP1*^{D868N}. Neither the *CSF3R*^{741*} truncation nor *CSF3R*^{WT} had colonies when expressed with empty vector, but a modest number of colonies were formed when combined with *SETBP1*^{D868N}.

Because transgenic models are not yet available for mutated *SETBP1*, we used retroviral vectors to study whether *SETBP1*^{D868N} augments *CSF3R*^{T618I}-driven oncogenesis in vivo. When 25 000 lineage-negative Balb/c bone marrow cells expressing *CSF3R*^{T618I} and/or *SETBP1*^{D868N} were transplanted into lethally irradiated mice along with 250 000 carrier cells, the mice with both mutations developed aggressive myeloid leukemia in <3 weeks (Figure 2A). This was associated with a rapid expansion of the granulocyte lineage, massive splenomegaly with a loss of splenic architecture, and moderate hepatomegaly (Figure 2B-I). There were no significant changes in terminal body weight (Figure 2J). Mice receiving bone marrow transplants expressing *SETBP1*^{D868N} alone had a median survival of 181 days, whereas mice receiving *CSF3R*^{T618I} alone did not reach their median survival during the course of this study (Figure 2A). A second transplantation was performed using bone marrow from Balb/c donors that had been treated with 5-fluorouracil to deplete mature progenitor cells. Transduced 5-fluorouracil–treated marrow was sorted, and 2000 cells per condition, along with 200 000 carrier marrow cells, were transplanted into lethally irradiated mice (supplemental Figure 2A). At day 19, mice were euthanized to collect flow cytometric end point on the bone marrow compartment. Mice with *CSF3R*^{T618I} plus *SETBP1*^{D868N} marrow had granulocytosis, with an expansion of Cd11b^{+} cells in the blood and bone marrow (supplemental Figure 2B-D).

Because coexpression of *CSF3R*^{T618I} and *SETBP1*^{WT} or *SETBP1*^{D868N} conferred replating potential in cytokine-free CFU assays, we hypothesized that these cells might also proliferate in liquid culture. Indeed, we found that *CSF3R*^{T618I} plus *SETBP1*^{WT}– and *CSF3R*^{T618I} plus *SETBP1*^{D868N}–expressing cells harvested from CFU assays grew in Iscove modified Dulbecco medium with 20% fetal bovine serum and no cytokine supplementation (supplemental Figure 3A-B). These cells could be maintained in culture for months with continued cell division and high viability. Neither gene alone conferred this growth potential (data not shown). *SETBP1* retroviral expression in this cell line was approximately threefold over baseline, comparable to the relative level of *SETBP1* overexpression in the top 5% of acute myeloid leukemia (AML) samples in the BeatAML cohort[29] (supplemental Figure 3C-D). Mouse bone marrow immortalized by *CSF3R*^{T618I} plus *SETBP1*^{D868N} was transplantable, producing a lethal leukemia with a median survival of ~4 weeks (supplemental Figure 3E-G).

To understand how *SETBP1* expression confers hemopoietic cell expansion in the context of *CSF3R*^{T618I}, we generated a new cell line in which expression of *SETBP1*^{D868N} was regulated by doxycycline (Figure 3A). Withdrawal of doxycycline from the cell culture media silenced expression of *SETBP1*^{D868N} and resulted in a cessation of cell growth after 48 hours and a sharp drop in viability at 72 hours (Figure 3B-C). At 24 hours, cells cultured with and without doxycycline had similar Cd11b and GR-1 expression,

Figure 1. *SETBP1* combines with *CSF3R* mutations to promote cellular proliferation in vitro. (A) To evaluate the effects of *SETBP1*^{WT}, *SETBP1*^{D868N}, and *CSF3R*^{T618I} or the combination of these mutations on hematopoietic progenitors, mouse bone marrow was retrovirally transduced to express mutations of interest or appropriate retroviral control vectors. Cells were then sorted based on fluorescent markers and plated in cytokine-free methylcellulose media in triplicate for a CFU assay. Representative images are shown here at day 7. (B) Quantification of the colony phenotype shown in panel A. Statistics: 2-way analysis of variance (ANOVA) with Tukey correction, shown for key relationships. Both the *CSF3R*^{T618I} plus *SETBP1*^{WT} and *CSF3R*^{T618I} plus *SETBP1*^{D868N} groups were significantly higher than every group with an empty vector ($P < .0001$). (C) Individual colonies were harvested from the methylcellulose using a glass pipette and spread onto a glass slide. Slides were then allowed to dry for 4 to 6 hours, stained with May-Grünwald and Giemsa solutions, and imaged. Representative images shown for cells expressing *CSF3R*^{T618I} with either *SETBP1*^{WT} or *SETBP1*^{D868N}. (D) After 7 days in culture, cells were harvested by diluting the methylcellulose with PBS and performing 3 PBS washes. Cells were counted using a TC20, and ~1250 cells per replicate per condition were plated into fresh cytokine-free methylcellulose media in triplicate. Serial replating was successful for at least 4 passages with both *CSF3R*^{T618I} plus *SETBP1*^{WT} and *CSF3R*^{T618I} plus *SETBP1*^{D868N}. (E) To evaluate if *SETBP1*^{D868N} enhanced colony formation driven by the endogenous ligand for CSF3R (granulocyte colony-stimulating factor [GCSF]), we plated 2000 *SETBP1*^{D868N}-expressing cells per well in cytokine-free methylcellulose media with or without exogenous GCSF (100 ng/mL). Representative images are shown. (F) Quantification of the CFU assay in panel E, with unpaired 2-tailed Student *t* test. (G) To determine if *SETBP1*^{D868N} enhances the CFU capacity of other *CSF3R* mutations, we transduced murine primary hematopoietic cells with either empty vector, *CSF3R*^{WT}, *CSF3R*^{741*}, *CSF3R*^{T618I}, or *CSF3R*$^{T618I/771fs}$ (green fluorescent protein [GFP]) along with either empty vector or *SETBP1*^{D868N} (red fluorescent protein [RFP]). Representative images are shown. (H) Quantification of the CFU assay in panel G, with 2-way ANOVA for simple effects within group and Tukey correction for multiple comparisons. *$P < .05$, **$P < .01$, ***$P < .001$, ****$P < .0001$.

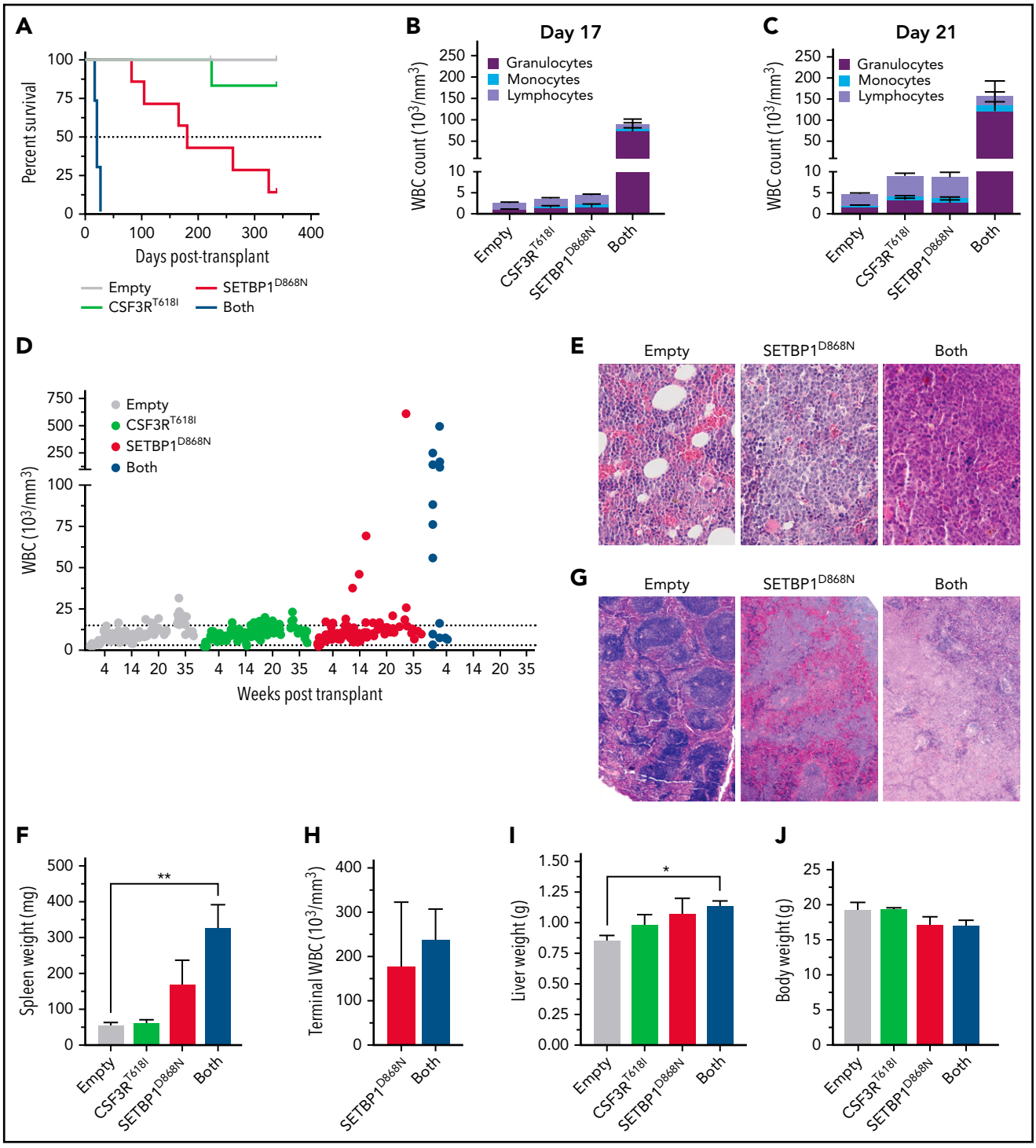

Figure 2. Transplantation of bone marrow cells expressing *CSF3R* and *SETBP1* mutations results in rapidly lethal leukemia. (A) Survival curves for *SETBP1* primary transplantation model. Transplantation of 25 000 lineage-negative *CSF3R*^{T618I} plus *SETBP1*^{D868N} cells, with 190 000 nontransfected carrier bone marrow cells, into lethally irradiated recipient mice resulted in rapidly lethal aggressive leukemia (n = 5-7). The median survival of *SETBP1*^{D868N} mice was 25.9 weeks. (B) Peripheral blood white blood cell (WBC) differentials at posttransplantation day 17. (C) Peripheral WBC differentials at day 21. (D) Peripheral WBC counts over time. (E) Representative hematoxylin and eosin (H&E)–stained tibia cross-sections showing increased cellularity at time of death with *SETBP1*^{D868N} alone and *CSF3R*^{T618I} plus *SETBP1*^{D868N}. (F) Terminal spleen weight. (G) Representative images of H&E-stained spleens showing splenic architecture changes. (H) Terminal WBC count. (I) Terminal liver weight. (J) Terminal body weight. Statistics: 1-way analysis of variance with Dunnett correction. *$P < .05$, **$P < .01$.

indicating they were in comparable myeloid differentiation states (Figure 3D-E). At 48 hours postdoxycycline withdrawal, there was a significant increase in the percentage of cells with high GR-1 expression, and there was a clear morphologic difference in the cells by histology (Figure 3E-G). Cells expressing only *CSF3R*^{T618I} (doxycycline negative) differentiated into mature myeloid cells, including neutrophil precursors and neutrophils with ring-shaped nuclei. This *CSF3R*^{T618I} plus *SETBP1*$^{D868N\text{-dox}}$ cell line model

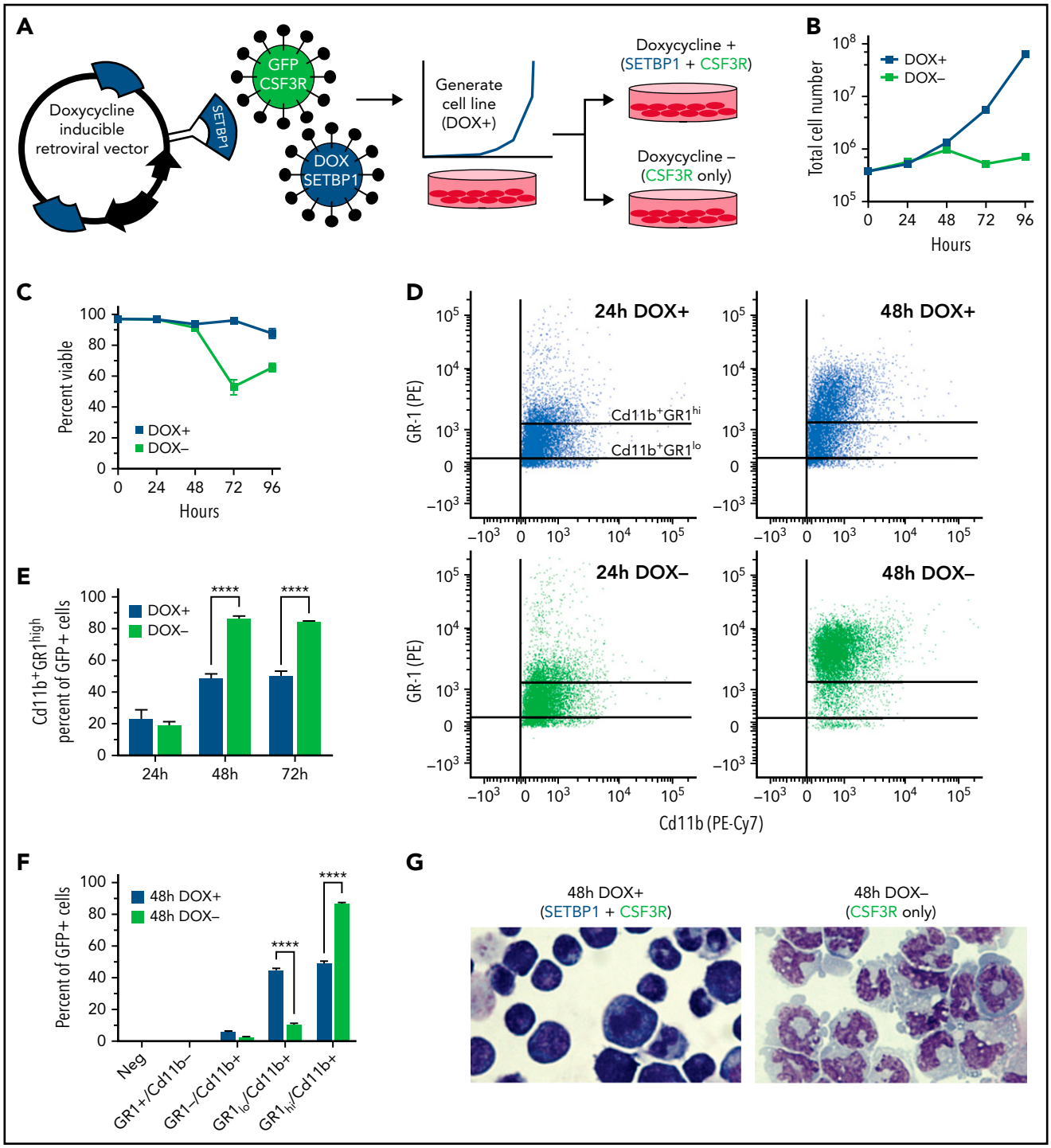

Figure 3. *CSF3R*^{T618I}- and *SETBP1*^{D868N}-expressing hematopoietic cells undergo cell-cycle arrest and differentiation after SETBP1 withdrawal. (A) Schematic of doxycycline (DOX)-inducible cell line generation (*CSF3R*^{T618I} plus *SETBP1*$^{D868N\text{-}dox}$). This cell line was generated from primary mouse bone marrow using retrovirally expressed oncogenes, with *CSF3R*^{T618I} in a constitutively active vector and *SETBP1*^{D868N} in a Tet-on vector. After transduction with both oncogenes, *CSF3R*$^{+}$ cells (green fluorescent protein positive [GFP^{+}]) were sorted and then cultured in the presence of DOX (1 μg/mL) to induce *SETBP1*^{D868N} expression. (B) Growth of *CSF3R*^{T618I} plus *SETBP1*$^{D868N\text{-}dox}$ cells with and without DOX. To shut off *SETBP1* expression, cells were washed with PBS 5 times and then resuspended in media with or without DOX in triplicate. Cells expressing only *CSF3R*^{T618I} stopped proliferating after 48 hours. (C) Cell death increased between 48 and 72 hours after *SETBP1* withdrawal. (D) Representative flow cytometric plots for Cd11b and GR1 expression at 24 and 48 hours postwithdrawal. After withdrawing DOX, cells were collected at 24-hour intervals to monitor changes in cell state. (E) Quantification of Cd11b^{+}GR1^{high} cells with and without DOX at 24, 48, and 72 hours. Statistics: repeated measures analysis of variance with multiple comparisons within time points [Šidák correction]. (F) Quantification of CD11b and GR1 at 48 hours, as gated in panel D. (G) Representative images of the cell line undergoing differentiation at 48 hours. ****$P < .0001$. PE, phycoerythrin.

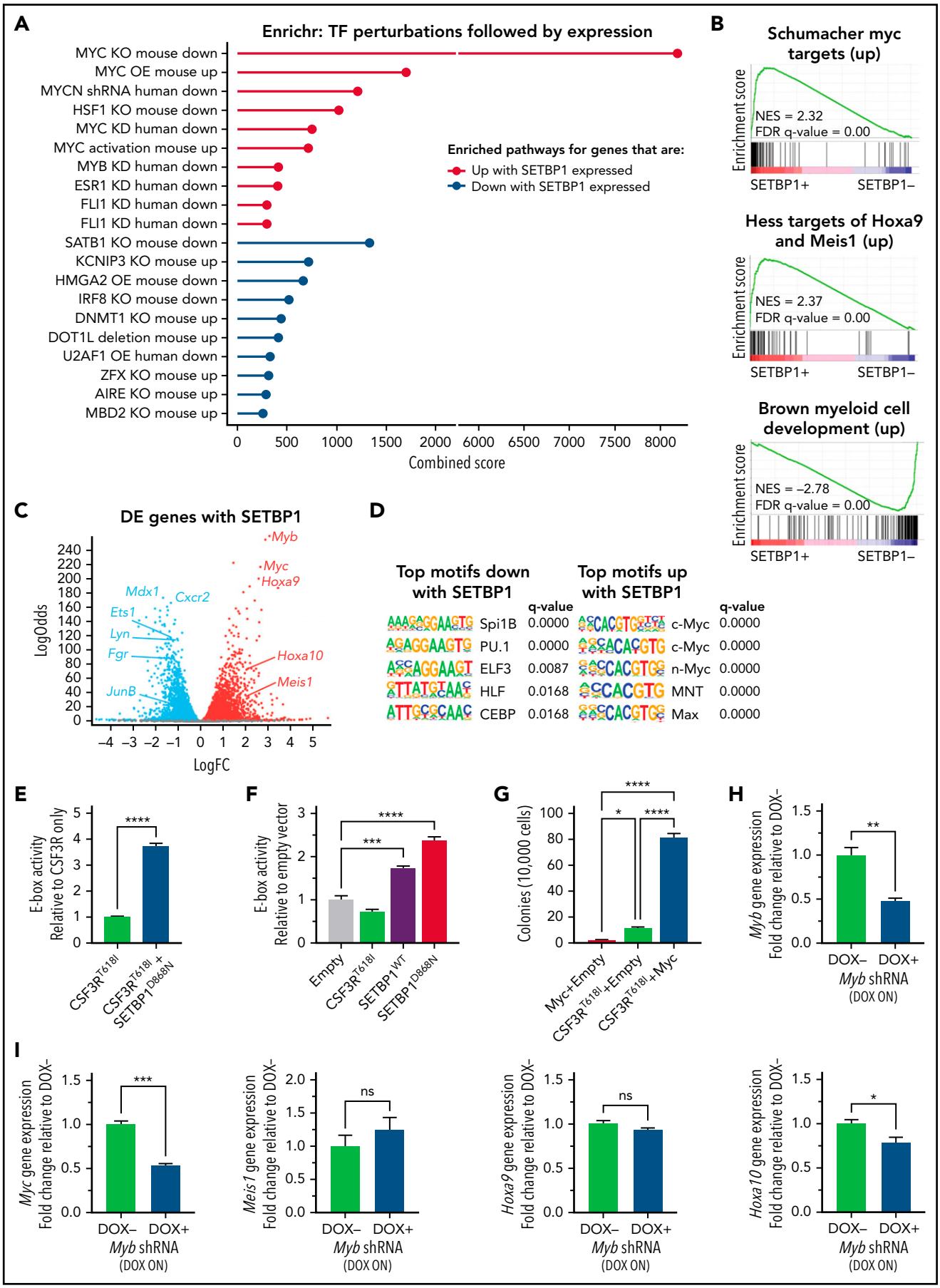

Figure 4.

provides a tractable system in which to evaluate SETBP1-driven molecular programs.

To identify transcriptional programs that are upregulated by *SETBP1*^{D868N} in the context of CNL, we performed RNA-seq of the *CSF3R*^{T618I} plus *SETBP1*$^{D868N\text{-dox}}$ cell line at 24 hours postdoxycycline withdrawal, when the cells were still viable and dividing, and compared them with cells treated with doxycycline. One of the strongest signatures in cells expressing *SETBP1*^{D868N} relative to those without *SETBP1*^{D868N} was that of MYC target genes (Figure 4A-D). Pathway analysis of the differentially expressed genes between *CSF3R*^{T618I} only (doxycycline negative) and *CSF3R*^{T618I} plus *SETBP1*^{D868N} (doxycycline positive) showed that pathways upregulated with *SETBP1*^{D868N} were overwhelmingly associated with MYC perturbations (Figure 4A). In the *CSF3R*^{T618I}-only condition, brown myeloid cell development differentiation–associated genes were enriched (Figure 4B). This is in line with our data showing that the *CSF3R*^{T618I}-only cells differentiated into mature myeloid cells between 24 and 48 hours postdoxycycline withdrawal (Figure 3D-F). Congruent with previous studies of SETBP1,[6-8,10] GSEA showed that SETBP1-associated genes were enriched for early progenitor pathways, including upregulated targets of Hoxa9 and Meis1 (Figure 4B). Consistent with the pathway analysis shown in Figure 4A, GSEA also identified that MYC targets were associated with *SETBP1*^{D868N} (Figure 4B). At the individual gene level, we found that *Myc*, *Meis1*, and *Hoxa9* themselves were highly upregulated (Figure 4C; supplemental Figure 4). Additionally, we saw that Hoxa10 and Myb, which have been previously associated with *SETBP1*-driven leukemogenesis,[6,10] were among the top differentially regulated genes when *SETBP1* was expressed (Figure 4C; supplemental Figure 4). Of note, *Myc* expression was not upregulated in an analogous *NRAS*^{G12D} plus *SETBP1*$^{D868N\text{-dox}}$ cell line (supplemental Figure 4F), indicating that there is context-specific manifestation of SETBP1 biology.

To determine if there are particular motifs enriched in regulatory regions of differentially expressed genes, we ran the HOMER motif discovery algorithm.[18] This analysis identified that the genes upregulated by *SETBP1*^{D868N} were enriched for genes regulated by MYC E-box motifs (Figure 4D). To validate this finding, we used a luciferase reporter driven by the MYC E-box element to measure if *SETBP1*^{D868N} modulates E-box activity. Congruent with the RNA-seq analysis, coexpression of *SETBP1*^{D868N} with *CSF3R*^{T618I} drove a 3.7-fold increase in MYC activity over *CSF3R*^{T618I} alone (Figure 4E). Independent of *CSF3R*^{T618I}, both *SETBP1*^{WT} and *SETBP1*^{D868N} increased MYC E-box activity by 1.7- and 2.4-fold, respectively (Figure 4F). Using a CFU assay, we demonstrated that the retroviral overexpression of *MYC* was sufficient to enhance *CSF3R*^{T618I}-driven colony formation (Figure 4G). Because SETBP1 upregulates Myb, which is known to promote the transcription of Myc in other contexts,[30] we set out to understand whether Myb is a critical mediator of SETBP1-driven Myc expression. We performed short hairpin RNA knockdown of *Myb* in a *CSF3R*^{T618I}/*SETBP1*^{D868N} cell line. Induction of the short hairpin RNA with doxycycline resulted in a 52% reduction in *Myb* expression (Figure 4H). Reduction in *Myb* expression resulted in a 47% decrease in *Myc* expression and a 22% decrease in *Hoxa10* (Figure 4I). Neither *Meis1* nor *Hoxa9*, 2 other key genes that are upregulated with SETBP1, were affected by *Myb* knockdown. This suggests the upregulation of *Myc* with *SETBP1*^{D868N} could occur at least in part through the upstream regulation of *Myb*.

To better understand the epigenetic changes associated with these differential gene expression programs, we performed CUT&Tag in the *CSF3R*^{T618I} plus *SETBP1*$^{D868N\text{-dox}}$ cell line for 3 histone marks: H3K4me1, H3K4me3, and H3K27Ac (Figure 5A). H3K4me1 is primarily associated with enhancers and H3K4me3 with promoters. H3K27Ac is associated with both active promoters and active enhancers. Although there was not a global change in deposition of these epigenetic marks, H3K4me3 and H3K27Ac differential peaks had enhanced MYC/MYB motif enrichment when *SETBP1*^{D868N} was expressed (supplemental Figure 5A-B; Figure 5B). Congruent with the RNA-seq data, MYC motifs were enriched in the peaks that were upregulated by SETBP1 (Figure 5B; supplemental Figure 5B). To relate histone modification marks to MYC genome binding activity, we used a public Myc chromatin immunoprecipitation–seq data set (ENCFF152JNC; Mus musculus strain MEL) and intersected Myc binding intervals with significant SETBP1-induced histone peaks (Figure 5C-E). Remarkably, 47% of the differential H3K4me3 peaks overlapped with Myc binding regions (756 of 1604 peaks), indicating an overlap in the promoters differentially regulated by Myc and SETBP1^{D868N} (Figure 5C). Representative tracks for 2 Myc targets at promoters are shown in Figure 5D. The overlap between differential H3K4me1 peaks and Myc targets was 15% (534 of 3453), and there was a 38% overlap for H3K27Ac and Myc (654 of 1724). For Myb-bound regions (ENCFF911NHJ; Mus musculus strain MEL), there were fewer regions of overlap: H3K4me3 (267 [17%] of 1604 peaks), H3K4me1 (308 [9%] of 3453), and H3K27Ac (299 [17%] of 1724; Figure 5E). We next set out to determine whether the aberrant programs might be pharmacologically reversible.

Figure 4. SETBP1 upregulates early progenitor gene expression pathways and is associated with increased activation of MYC targets. (A) Top Enrichr transcription factor perturbation followed by expression pathways for genes that are differentially expressed with *SETBP1*. We performed RNA-seq on the *CSF3R*^{T618I} plus *SETBP1*$^{D868N\text{-dox}}$ cell line at 24 hours postdoxycycline (DOX) withdrawal, when the cells were still viable and dividing. Data are reported for cells with DOX (*CSF3R*^{T618I} plus *SETBP1*$^{D868N\text{-ON}}$) relative to those without DOX (*CSF3R*^{T618I} plus *SETBP1*$^{D868N\text{-OFF}}$). Enrichr calculates the combined score by multiplying the pathway *z* score and log(*P* value). (B) GSEA was performed to identify pathways that are enriched with *SETBP1* expression. Three of the top GSEA plots, each with a false-discovery rate (FDR) *q* value of 0.00, are shown. (C) Glimma volcano plot showing differentially expressed genes with *SETBP1*^{D868N}, with several key genes annotated. (D) HOMER motif analysis was run to identify the top motifs enriched in the genes differentially upregulated and downregulated by SETBP1. (E) Coexpression of *SETBP1*^{D868N} with *CSF3R*^{T618I} drove a 3.7-fold increase in MYC activity over *CSF3R*^{T618I} alone. A luciferase reporter assay for the MYC E-box was used to measure if *SETBP1*^{D868N} modulates E-box activity. Using an MYC E-box reporter plasmid, E-box activity was measured in transfected 293T17 cells expressing *CSF3R*^{T618I} alone or *CSF3R*^{T618I} plus *SETBP1*^{D868N}. (F) In transfected 293T17 cells expressing only *CSF3R*^{T618I}, *SETBP1*^{WT}, or *SETBP1*^{D868N}, *CSF3R* did not increase E-box activity above baseline, whereas both WT and mutated *SETBP1* significantly increased E-box activity. (G) Coexpression of *MYC* with *CSF3R*^{T618I} in a CFU assay resulted in an increase in colony formation over either oncogene alone. A colony forming unit assay was performed to assess whether expression of *MYC* is sufficient to increase *CSF3R*-driven colony formation. A total of 10 000 cells expressing either *MYC*, *CSF3R*^{T618I}, or both were plated in cytokine-free methylcellulose, and CFUs were counted after 7 days. (H) An inducible lentiviral *Myb* short hairpin RNA (shRNA) construct was stably expressed in the *CSF3R*^{T618I} plus *SETBP1*^{D868N} cell line. Addition of DOX to the media knocked down *Myb* expression by ~52%. (I) Knockdown (KD) of *Myb* resulted in a 47% decrease in *Myc* expression and a 22% decrease in *Hoxa10* but no significant changes to *Meis1* or *Hoxa9*. *$P < .05$, **$P < .01$, ***$P < .001$, ****$P < .0001$. FC, fold change; KO, knockout; NES, normalized enrichment score; ns, not significant; OE, overexpression.

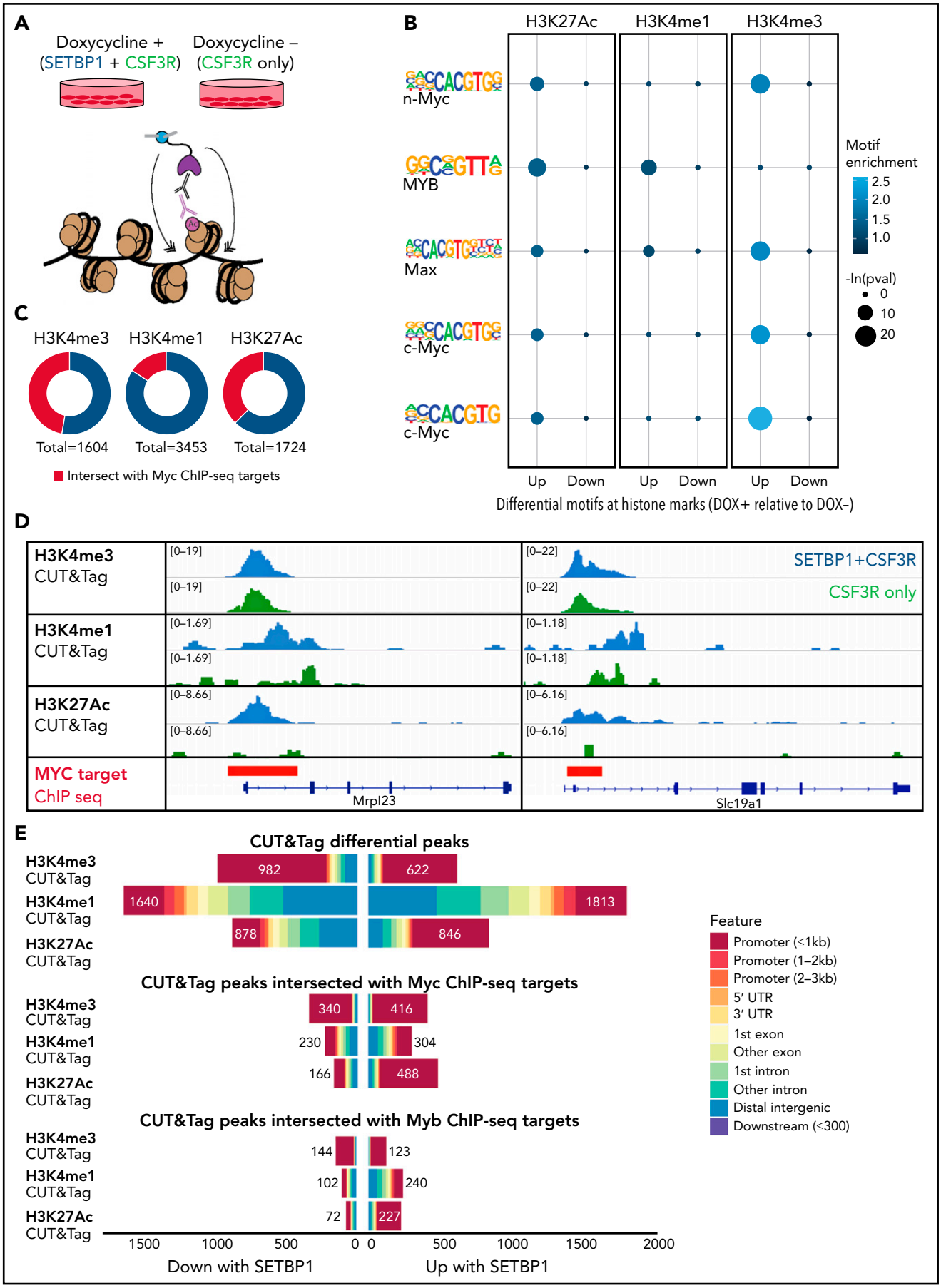

Figure 5.

To determine the essential cell growth and survival pathways in *SETBP1*-mutated cells, we performed a chemical screen with 175 inhibitors with known sensitivity in patient samples (BeatAML cohort[29]). The median 50% inhibitory concentration (IC_{50}) for each inhibitor in the BeatAML cohort[29] was divided by the IC_{50} for the same inhibitor in the *CSF3R*^{T618I} plus *SETBP1*^{D868N} cell line (2 biologic replicate lines; technical triplicates) to calculate a fold increase in sensitivity relative to other samples. This enabled us to examine to which drugs this sample is particularly sensitive, as opposed to drugs that are generally toxic. Consistent with the activation of the JAK/STAT pathway by mutated *CSF3R*, this cell line was sensitive to JAK inhibitors. Annotations for the top 15 inhibitors are listed in supplemental Tables 1 and 2. Interestingly, the top 2 hits were LSD1 inhibitors (Figure 6A; supplemental Figure 6A). Recently, it was reported that *Flt3*^{ITD}-mutated AML cells overexpressing *SETBP1*, which have a similar profile of overexpressed genes to our *CSF3R*^{T618I} plus *SETBP1*^{D868N} cell line (*Meis1*, *Kdm1a*, *Mecom*, *Gfi1*, *Myc*, *Myb*, and *Bcl2*), were sensitive to LSD1 inhibitors.[31] Additionally, a previous study found that LSD1 induces *Myc* transcriptional activity in a nonhematopoietic context.[32] We were therefore interested in whether LSD1 inhibitors could reduce aberrant MYC activity driven by SETBP1. Using a luciferase promoter assay, we determined that MYC E-box activity was modulated by LSD1 inhibition and found a modest dose-dependent response to GSK2879552, culminating in a 24% reduction in E-box activity at 250 nM (Figure 6B). We next tested a third LSD1 inhibitor, GSK-LSD1, which proved to be more potent in this cell line, with an IC_{50} of ~250 nM compared with 590 nM (supplemental Figure 6B).

Although the *CSF3R*^{T618I} plus *SETBP1*^{D868N} cell line was sensitive to the LSD1 inhibitors, cell death occurred at higher doses (>100 nM). Given this, we were interested in understanding whether LSD1 treatment could modulate SETBP1-driven oncogenic programs and if lower doses could potentially sensitize cells to other therapies. To determine whether LSD1 inhibition reduces *Myc* gene expression to basal levels, we used the *CSF3R*^{T618I} plus *SETBP1*$^{D868N\text{-dox}}$ cell line. To determine basal gene expression, *SETBP1*^{D868N} expression was silenced by withdrawing doxycycline in triplicate. In parallel, *CSF3R*^{T618I} plus *SETBP1*$^{D868N\text{-dox}}$ cells were cultured in the presence of doxycycline and treated in triplicate with either DMSO, JQ1, GSK2879552, or GSK-LSD1. After 48 hours, cells were harvested to assess *Myc* expression by qPCR. Treatment with the bromodomain inhibitor JQ1, which has been shown to reduce *Myc* expression in some contexts, yielded no significant changes to *Myc* expression in this molecular context. However, both LSD1 inhibitors reduced *Myc* expression significantly (Figure 6C). Using the cell line that constitutively expresses *CSF3R*^{T618I} plus *SETBP1*^{D868N}, we then evaluated how lower doses of LSD1 inhibition (100 nM of GSK2879552, 30 nM of GSK-LSD1, or 30 nM of ORY-1001) modulated 4 key SETBP1-associated genes: *Myc*, *Myb*, *Meis1*, and *Hoxa9*. In the *CSF3R*^{T618I} plus *SETBP1*^{D868N} cells, LSD1 inhibitors reduced *Myc*, *Myb*, and *Meis1* expression but did not significantly decrease *Hoxa9* expression after 48 hours of treatment (Figure 6D-G). Of note, another inhibitor of LSD1 under investigation in clinical trials, ORY-1001, was remarkably effective, reducing *Myc*, *Myb*, and *Meis1* expression by ~80% to 90%. To assess global transcriptional changes with LSD1 inhibition, we performed RNA-seq on cells treated with either 100 nM of GSK2879552 or 30 nM of ORY-1001 for 24 hours. Using GSEA, we found that LSD1 inhibition was inversely associated with MYC target amplification; MYC targets were enriched in the DMSO-treated cells relative to the LSD1-treated cells (Figure 6H).

Samples from patients with CNL are rare and can exhibit low viability after cryopreservation as a result of the abundance of neutrophils in the peripheral blood and bone marrow. To assess whether LSD1 inhibition can modulate progenitor populations and MYC signaling in a human patient sample, we isolated viable CD34$^+$ progenitor cells from a *CSF3R*^{T618I} plus *SETBP1*^{G870S} cryopreserved CNL bone marrow sample and cultured these CD34$^+$ cells in a serum-free expansion media for 7 days. The total number of CD34$^+$ cells expanded from 65 400 to 642 000 cells in 7 days. A total of 300 000 cells were then treated with 100 nM of either ORY-1001 or DMSO for 24 hours. After treatment, single-cell RNA-seq with barcoded antibody labeling (CITE-seq) was performed. Marker genes (*MPO*, *GATA1*, *GATA2*, *IRF8*, *ELANE*, *LYZ*, and *CEBPE*) and surface antigens (CD34 and CD45RA) were used for population identification (Figure 6I; supplemental Figure 7). We found that ORY-1001 treatment significantly decreased *MYC* expression in hematopoietic progenitor clusters expressing high levels of CD34 (Figure 6I).

The JAK inhibitor ruxolitinib is under investigation as a promising therapeutic agent for patients who have mutations in *CSF3R* and has shown efficacy in a clinical trial.[2] To improve initial treatment response rates and circumvent resistance, it is likely that a multipronged therapeutic approach will be needed. From our chemical screen in the *CSF3R*^{T618I} plus *SETBP1*^{D868N} cell line, we knew that these cells are sensitive to JAK inhibitors relative to the median IC_{50} for patient samples in the BeatAML cohort[29] (Figure 6A). To evaluate how *SETBP1*^{D868N} alters sensitivity to ruxolitinib, we performed a 7-day cytokine-free colony assay with mouse bone marrow retrovirally transduced with either *CSF3R*^{T618I} plus empty vector or *CSF3R*^{T618I} plus *SETBP1*^{D868N} (supplemental Figure 8A). Cells were plated with increasing concentrations of ruxolitinib and found to have less sensitivity with *CSF3R*^{T618I} plus *SETBP1*^{D868N} (IC_{50}, 296 nM) than with *CSF3R*^{T618I} plus empty vector (IC_{50}, 78 nM). The IC_{50} of primary *CSF3R*^{T618I} plus *SETBP1*^{D868N}–transduced cells in colony assay was similar to that of the *CSF3R*^{T618I} plus *SETBP1*^{D868N} cell line (241 nM; supplemental Figure 8B).

Figure 5. Epigenetic regulation of MYC targets by SETBP1. (A) Schematic: we performed CUT&Tag in our *CSF3R*^{T618I} plus *SETBP1*$^{D868N\text{-dox}}$ cell line for 3 histone marks. Doxycycline (DOX) was withdrawn from the cell line to turn off oncogenic *SETBP1* expression, and cells were harvested for epigenetic analyses at 24 hours post-withdrawal. (B) MYC family motifs identified for each histone mark at differential peaks between DOX$^+$ and DOX$^-$ conditions. Motif enrichment shown for DOX$^+$ relative to DOX$^-$. (C) Regions of significant SETBP1-induced histone peaks were intersected with MYC (ENCFF152JNC). (D) Representative tracks are shown here for each histone mark at the location of an MYC target identified using MYC chromatin immunoprecipitation (ChIP)–seq data from ENCODE (ENCFF152JNC). (E) Features plots for differential peaks showing the breakdown of peaks within promoters and other elements. Regions of significant SETBP1-induced histone peaks were intersected with either MYC (ENCFF152JNC) or MYB (ENCFF911NHJ) ChIP-seq data. The total number of differential peaks for each condition is annotated. UTR, untranslated region.

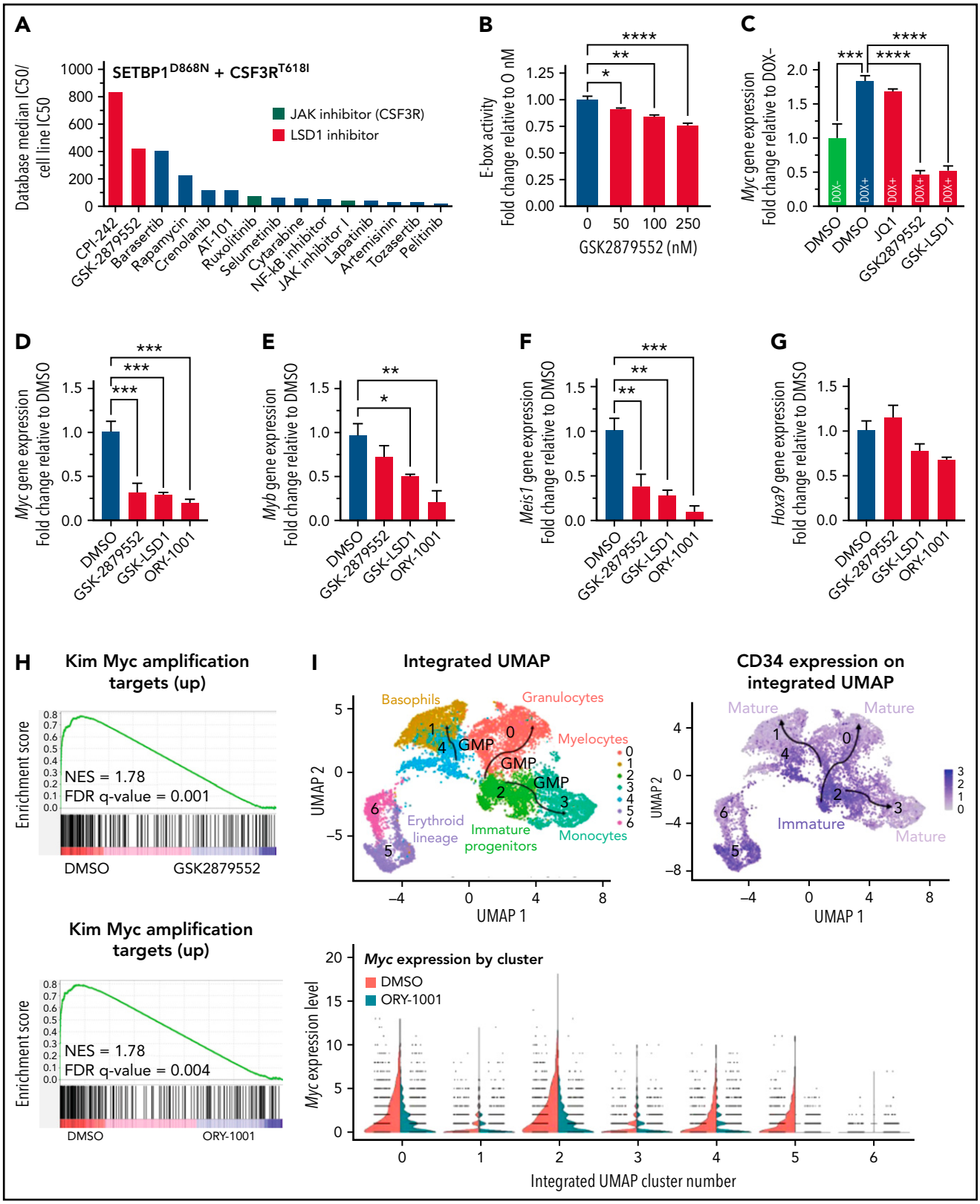

Figure 6. LSD1 inhibitors normalize aberrant SETBP1 transcriptional programs. (A) A medium-throughput inhibitor screen was performed on the *CSF3R*^{T618I} plus *SETBP1*^{D868N} cell line, and both LSD1 inhibitors and JAK inhibitors were among the top hits. The 175 inhibitors evaluated have known sensitivity in patient samples (BeatAML cohort[29]). The inhibitors were ranked for this analysis by dividing the median IC_{50} of all samples previously screened by our cell line IC_{50} to determine a fold change. (B) A luciferase E-box activity assay was performed with 4 concentrations of the LSD1 inhibitor GSK2879552. In 293T17 cells expressing *CSF3R*^{T618I} and *SETBP1*^{D868N}, LSD1 inhibition reduced MYC activity by 24% at 250 nM. (C) In our cell line where *SETBP1*^{D868N} expression was regulated by doxycycline (DOX), we evaluated whether LSD1 inhibitors would reduce *Myc* gene expression to the level of DOX^{-} cells. The LSD1 inhibitors GSK2879552 (1000 nM) and GSK-LSD1 (100 nM) both reduced *Myc* expression in *CSF3R*^{T618I} plus *SETBP1*^{D868N} cells, but JQ1 (200 nM) did not. (D) qPCR for *Myc* was performed after treatment of the *CSF3R*^{T618I} plus

To determine whether LSD1 inhibitors, which reduce SETBP1-associated aberrant gene expression, are effective in combination with JAK inhibitors, we next evaluated the synergy between these 2 agents (Figure 7A; supplemental Figure 8C). Each LSD1 inhibitor that we tested exhibited marked synergy with ruxolitinib, with the greatest synergy observed with ORY-1001 (δ score, 22.028). To understand the mechanisms underlying this drug synergy, RNA-seq was performed on cells treated with DMSO, ruxolitinib, GSK2879552, ORY-1001, ruxolitinib with GSK2879552, or ruxolitinib with ORY-1001. A heat map was generated using unbiased clustering, and the individual clusters were analyzed using HOMER motif enrichment and Enrichr pathway analysis (Figure 7B). In cluster 1, we saw genes that were upregulated by the combination therapy more than by either drug alone. Motifs for cluster 1 included differentiation-associated transcription factors PU.1 and Runx1, which are both members of the core binding factor complex. Cluster 4 contained genes that were downregulated more by the combination than by either drug alone. In this cluster, we saw an Myc and Fli1 signature. When mice receiving transplants of the *CSF3R*^{T618I} plus *SETBP1*^{D868N} cell line were treated with an LSD1 inhibitor (0.75 mg/kg of GSK2887552 twice per day) and ruxolitinib (90 mg/kg twice per day), survival was significantly improved, without any significant measures of antiplatelet toxicity (Figure 7C-E; supplemental Figure 9A). Bone marrow cellularity was lower at the time of death in mice receiving the combination (supplemental Figure 9B). This supports a model whereby LSD1 inhibition reverses SETBP1-associated phenotypes and provides rationale for combined LSD1/JAK therapeutic strategies for leukemia with *CSF3R* and *SETBP1* mutations.

Discussion

SETBP1 is recurrently mutated in myeloid malignancies, including atypical chronic myeloid leukemia, chronic myelomonocytic leukemia, and juvenile myelomonocytic leukemia. *SETBP1* mutations occur at a particularly high frequency in CNL, a leukemia characterized by *CSF3R* mutations and the overproduction of neutrophils. The primary goal of this study was to determine how *SETBP1* mutations contribute to the pathobiology of *CSF3R*-driven leukemias. We found that *SETBP1*^{WT} and *SETBP1*^{D868N} each dramatically increased *CSF3R*^{T618I}-driven hematopoietic progenitor proliferation and accelerated *CSF3R*^{T618I}-driven disease (Figures 1-3). Expression of *SETBP1*^{D868N} led to upregulation of progenitor-associated gene expression programs and downregulation of differentiation-associated genes. *SETBP1*^{D868N}-driven Myc expression could be reversed by treatment of cells with LSD1 inhibitors. Furthermore, LSD1 inhibition synergized with inhibition of *CSF3R*^{T618I}-driven signaling in these models.

In the context of a *CSF3R* mutation, we found that mutated *SETBP1* increased *Hoxa9*, *Hoxa10*, *Meis1*, and *Myb* transcript levels and increased their associated gene expression programs (Figure 4). This is congruent with previous studies establishing Setbp1 as a transcriptional regulator of Hox genes[6,10,33] and *Myb*.[10,33] An exciting finding of our transcriptional and epigenetic analyses was that expression of *SETBP1*^{D868N} was also associated with a strong Myc pathway signature (Figures 4 and 5). Myc is a transcription factor that plays an integral role in establishing a balance between self-renewal and hematopoietic differentiation.[34] The differentiation block and increased proliferation that occurred with *SETBP1*^{D868N} in the *CSF3R*^{T618I} plus *SETBP1*$^{D868N\text{-dox}}$ model are consistent with the known role of Myc in the inhibition of differentiation in other leukemia models.[34] Coexpression of *MYC* with *CSF3R*^{T618I} in a CFU assay largely recapitulated the dense and proliferative colony phenotype associated with the combination of *CSF3R*^{T618I} and *SETBP1*^{D868N} (Figure 4). This demonstrates that *MYC* overexpression is sufficient for recapitulation of the proliferative phenotype associated with *SETBP1* mutations. Knockdown of *Myb* in the *CSF3R*^{T618I} plus *SETBP1*^{D868N} cell line resulted in a significant decrease in *Myc* expression, indicating regulation of Myc programs might be mediated by *SETBP1*-driven Myb overexpression (Figure 4).

Although we know that ruxolitinib can be efficacious in CNL, it is likely that additional agents will be needed to achieve long-term remissions.[2] In our study, we found that although cells with both *CSF3R* and *SETBP1* mutations retained sensitivity to ruxolitinib, cells expressing both mutations had less sensitivity than those with *CSF3R*^{T618I} alone (supplemental Figure 8). We hypothesized that if *SETBP1*^{D868N} drives aggressive disease biology through epigenetic dysregulation of Myc regulatory elements, then therapeutic strategies that normalize *Myc* expression will be effective against *SETBP1*-mutated leukemia. We found that LSD1 inhibition decreased cell viability and suppressed aberrant *Myc* expression (Figure 6). In a sample from a patient with *SETBP1*-mutated CNL, LSD1 inhibitor treatment significantly decreased *Myc* expression in CD34-high hematopoetic progenitor clusters (Figure 6I). Having established that LSD1 inhibition reduces *SETBP1*-driven Myc expression, we next tested whether it might be useful in combination with the JAK1/2 inhibitor ruxolitinib. Each of the 3 LSD1 inhibitors tested demonstrated synergy with ruxolitinib (Figure 7A). To understand the mechanism of synergy, we performed RNA-seq analysis. This revealed a group of genes downregulated by the combination (Figure 7B; cluster 4). Myc was the most prominent motif in this downregulated cluster, and Myc motifs had a high degree of enrichment in this cluster relative to all other clusters. Furthermore, Enrichr pathway analysis revealed a significant repression of Myc-regulated pathways. Additionally, the RNA-seq analysis revealed that this drug synergy was associated with the reactivation of differentiation-associated pathways. A previous study of *CSF3R*/*CEBPA*-mutated AML demonstrated that LSD1 inhibition caused marked reactivation of differentiation-associated enhancers.[35] In our model, genes upregulated by the combination of LSD1 and JAK inhibition were enriched for PU.1 and Runx1 motifs (Figure 7B; cluster 1). These findings are in line with previous studies of LSD1 inhibition in leukemia showing activation of PU.1 targets in *MLL*-rearranged AML[36,37] and *KIT*-mutated AML.[38] It is not clear if the repression of stem/progenitor programs is a direct effect

Figure 6 (continued) *SETBP1*^{D868N} cell line with 1 of 3 LSD1 inhibitors at 100 nM (GSK2879552) or 30 nM (GSK-LSD1 and ORY-1001) for 48 hours. (E) qPCR for *Myb*. (F) qPCR for *Meis1*. (G) qPCR for *Hoxa9*, which is not modulated by LSD1 inhibition at these concentrations. (H) RNA-seq was performed after treatment of the cell line with 100 nM of GSK2879552 or 30 nM of ORY-1001 for 24 hours. GSEA demonstrated that this treatment was associated with a reversal of MYC amplification with both inhibitors. (I) A *CSF3R*^{T618I}- and *SETBP1*^{G870S}-mutated patient sample was treated with 100 nM of ORY-1001 for 24 hours, and CITE-seq (single-cell RNA-seq with barcoded antibody labeling) was performed. Treatment significantly decreased *Myc* expression in hematopoietic progenitor clusters expressing high levels of CD34. *$P < .05$, **$P < .01$, ***$P < .001$, ****$P < .0001$. FDR, false-discovery rate; NES, normalized enrichment score.

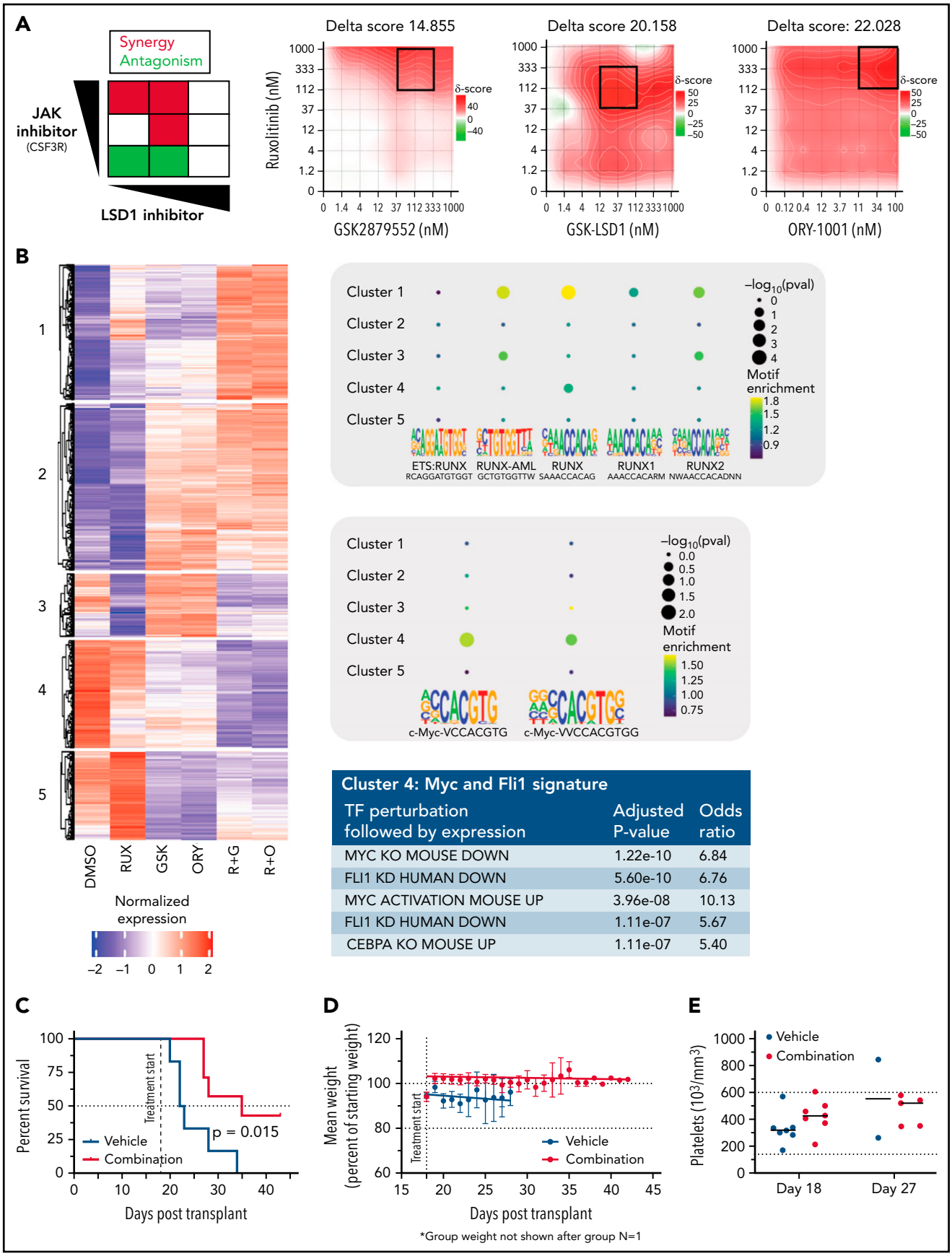

Cluster 4: Myc and Fli1 signature

TF perturbation followed by expression	Adjusted P-value	Odds ratio
MYC KO MOUSE DOWN	1.22e-10	6.84
FLI1 KD HUMAN DOWN	5.60e-10	6.76
MYC ACTIVATION MOUSE UP	3.96e-08	10.13
FLI1 KD HUMAN DOWN	1.11e-07	5.67
CEBPA KO MOUSE UP	1.11e-07	5.40

Figure 7.

of LSD1 inhibition or a secondary effect of promotion of a more differentiated phenotype. When the combination of GSK287552 and ruxolitinib was evaluated in an in vivo model of *CSF3R*^{T618I}/*SETBP1*^{D868N} leukemia, there was a significant increase in survival over the vehicle-treated mice (Figure 7C). Both JAK inhibitors and LSD1 inhibitors have been tested in clinical trials for myeloid malignancies as single agents, with limiting toxicities. In this model, the combination therapy was well tolerated, and there was no decrease in platelets with the combination treatment (Figure 7D-E).

In summary, we investigated the role of *SETBP1* mutations in *CSF3R*-driven leukemia. We found that *SETBP1* mutations accelerated leukemic progression in mice. When a *SETBP1* mutation was expressed in murine hematopoietic cells along with a *CSF3R* mutation, *SETBP1* promoted proliferation of immature granulocytes through upregulation of the Myc pathway and epigenetic modulation of Myc target genes. Treatment of *CSF3R*- and *SETBP1*-mutated cells with ruxolitinib (targeting *CSF3R* signaling) and an epigenetic modulatory drug resulted in synergistic cell death and a repression of aberrant transcriptional programs. These data contribute to our understanding of how *SETBP1* mutations augment *CSF3R*-driven oncogenic programs to produce lethal disease and provide preclinical evidence for a combination therapeutic strategy in *CSF3R*- and *SETBP1*-mutated leukemia.

Acknowledgments

The authors thank the following Oregon Health & Science University core facilities for their assistance: Advanced Light Microscopy, Flow Cytometry Shared Resource, ExaCloud Cluster Computational Resource, and Advanced Computing Center.

Research reported in this publication was supported by an American Society of Hematology Research Restart Award, a Collins Medical Trust Award, a Medical Research Foundation Early Clinical Investigator Award, and National Cancer Institute (NCI), National Institutes of Health, grant F32CA239422 (S.A.C.); an American Society of Hematology Research Restart Award, an American Society of Hematology Scholar Award, and NCI grant 1 K08 CA245224 (T.P.B.); a Knight Pilot Award, an American Society of Hematology Junior Faculty Scholar Award, the Gilead Research Scholars Program in Hematology/Oncology, and XXX grant 1R01HL157147-01 (J.E.M.).

Authorship

Contribution: S.A.C., B.J.D., T.P.B., and J.E.M. were responsible for conception and design. S.A.C., B.M.C., B.N.M., H.Z.B., A.B., T.P.B., and J.E.M. performed in vitro experiments. S.A.C., Z.S., and L.M. performed in vivo experiments. G.L.K., B.M.C., and T.P.B. provided computational resources. S.A.C., G.L.K., B.M.C., B.N.M., H.Z.B., B.J.D., T.P.B., and J.E.M. analyzed and interpreted the data. All authors wrote, reviewed, and revised the manuscript.

Conflict-of-interest disclosure: B.J.D. has potential competing interests as follows: scientific advisory board (SAB) for Aileron Therapeutics, Therapy Architects (ALLCRON), Cepheid, Vivid Biosciences, Celgene, RUNX1 Research Program, EnLiven Therapeutics, Gilead Sciences (inactive), and Monojul (inactive); SAB for and stock ownership in Aptose Biosciences, Blueprint Medicines, Iterion Therapeutics, Third Coast Therapeutics, and GRAIL (SAB inactive); scientific founder of MolecularMD (inactive; acquired by ICON); board of directors for and stock ownership in Amgen; board of directorsfor Burroughs Wellcome Fund and CureOne; joint steering committee for Beat AML LLS; founder of VB Therapeutics; clinical trial funding from Novartis, Bristol-Myers Squibb, and Pfizer; and royalties from patent 6958335 (Novartis exclusive license) and Oregon Health & Science University and Dana-Farber Cancer Institute (one Merck exclusive license). J.E.M. reports the following: collaboration with Ionis pharmaceuticals and research funding from Gilead Sciences. The remaining authors declare no competing financial interests.

ORCID profiles: S.A.C., 0000-0003-2493-6789; G.L.K., 0000-0001-5262-5406; B.M.C., 0000-0002-5274-8323; Z.S., 0000-0001-9643-3588; L.M., 0000-0001-9582-3525; B.N.M., 0000-0001-9205-7423; H.Z.B., 0000-0002-0606-502X; A.B., 0000-0002-4091-9711; B.J.D., 0000-0001-8331-8206.

Correspondence: Julia E. Maxson, Oregon Health & Science University, Mail code KR-HEM, 3181 S.W. Sam Jackson Park Rd, Portland, OR 97239; e-mail: maxsonj@ohsu.edu.

Footnotes

Submitted 24 November 2021; accepted 15 April 2022; prepublished online on *Blood* First Edition 28 April 2022. DOI 10.1182/blood.2021014777.

Contact Julia E. Maxson at maxsonj@ohsu.edu for information regarding renewable materials, data sets, and protocols. Genomic data are accessible at National Center for Biotechnology Information Gene Expression Omnibus database (GSE189502).

The online version of this article contains a data supplement.

There is a *Blood* Commentary on this article in this issue.

The publication costs of this article were defrayed in part by page charge payment. Therefore, and solely to indicate this fact, this article is hereby marked "advertisement" in accordance with 18 USC section 1734.

Figure 7. XXX. (A) Synergy between each LSD1 inhibitor and ruxolitinib, with the greatest synergy between ORY-1001 and ruxolitinib (δ score, 22.028). To determine if there is synergy between LSD1 inhibition targeting SETBP1-driven pathways and a JAK1/2 inhibitor (ruxolitinib) targeting CSF3R-driven pathways, the *CSF3R*^{T618I} plus *SETBP1*^{D868N} cell line was plated in an 8 × 8 matrix in triplicate with increasing concentrations of each inhibitor. (B) RNA-seq data from cells treated with DMSO, 100 nM of ruxolitinib, 100 nM of GSK2879552 (GSK), 30 nM of ORY-1001, ruxolitinib with GSK2879552 (R+G), or ruxolitinib with ORY-1001 (R+O). Cluster 1 represents pathways upregulated more by the combination therapy than by either drug alone and includes a number of differentiation-associated transcription factors. Cluster 4 represents pathways downregulated more by the combination than by either drug alone and has an Myc and Fli1 signature. (C) Mice receiving transplants of the *CSF3R*^{T618I} plus *SETBP1*^{D868N} cell line were treated with 90 mg/kg of ruxolitinib twice per day and 0.75 mg/kg of GSK2879552 twice per day to determine if the combination treatment would improve survival over vehicle. Kaplan-Meier survival plot showing significant increase in survival with combination. (D) Mean mouse body weight during course of treatment with vehicle or combination. (E) Platelet counts at start of treatment (day 18) and midway through treatment course (day 27). Platelets did not decrease with combination treatment and remained within normal parameters. KD, knockdown; KO, knockout.

REFERENCES

1. Maxson JE, Gotlib J, Pollyea DA, et al. Oncogenic CSF3R mutations in chronic neutrophilic leukemia and atypical CML. *N Engl J Med.* 2013;368(19):1781-1790.
2. Dao KT, Gotlib J, Deininger MMN, et al. Efficacy of ruxolitinib in patients with chronic neutrophilic leukemia and atypical chronic myeloid leukemia. *J Clin Oncol.* 2020;38(10):1006-1018.
3. Piazza R, Valletta S, Winkelmann N, et al. Recurrent SETBP1 mutations in atypical chronic myeloid leukemia. *Nat Genet.* 2013;45(1):18-24.
4. Shou LH, Cao D, Dong XH, et al. Prognostic significance of SETBP1 mutations in myelodysplastic syndromes, chronic myelomonocytic leukemia, and chronic neutrophilic leukemia: A meta-analysis. *PLoS One.* 2017;12(2):e0171608.
5. Cristóbal I, Blanco FJ, Garcia-Orti L, et al. SETBP1 overexpression is a novel leukemogenic mechanism that predicts adverse outcome in elderly patients with acute myeloid leukemia. *Blood.* 2010;115(3):615-625.
6. Oakley K, Han Y, Vishwakarma BA, et al. Setbp1 promotes the self-renewal of murine myeloid progenitors via activation of Hoxa9 and Hoxa10. *Blood.* 2012;119(25):6099-6108.
7. Piazza R, Magistroni V, Redaelli S, et al. SETBP1 induces transcription of a network of development genes by acting as an epigenetic hub. *Nat Commun.* 2018;9(1):2192.
8. Vishwakarma BA, Nguyen N, Makishima H, et al. Runx1 repression by histone deacetylation is critical for Setbp1-induced mouse myeloid leukemia development. *Leukemia.* 2016;30(1):200-208.
9. Minakuchi M, Kakazu N, Gorrin-Rivas MJ, et al. Identification and characterization of SEB, a novel protein that binds to the acute undifferentiated leukemia-associated protein SET. *Eur J Biochem.* 2001;268(5):1340-1351.
10. Nguyen N, Vishwakarma BA, Oakley K, et al. Myb expression is critical for myeloid leukemia development induced by Setbp1 activation. *Oncotarget.* 2016;7(52):86300-86312.
11. Carratt SA, Braun TP, Coblentz C, et al. Mutant SETBP1 enhances NRAS-driven MAPK pathway activation to promote aggressive leukemia. *Leukemia.* 2021;35(12):3594-3599.
12. Bolger AM, Lohse M, Usadel B. Trimmomatic: a flexible trimmer for Illumina sequence data. *Bioinformatics.* 2014;30(15):2114-2120.
13. Dobin A, Davis CA, Schlesinger F, et al. STAR: ultrafast universal RNA-seq aligner. *Bioinformatics.* 2013;29(1):15-21.
14. Chen EY, Tan CM, Kou Y, et al. Enrichr: interactive and collaborative HTML5 gene list enrichment analysis tool. *BMC Bioinformatics.* 2013;14:128.
15. Kuleshov MV, Jones MR, Rouillard AD, et al. Enrichr: a comprehensive gene set enrichment analysis web server 2016 update. *Nucleic Acids Res.* 2016;44(W1):W90-W97.
16. Mootha VK, Lindgren CM, Eriksson KF, et al. PGC-1alpha-responsive genes involved in oxidative phosphorylation are coordinately downregulated in human diabetes. *Nat Genet.* 2003;34(3):267-273.
17. Subramanian A, Tamayo P, Mootha VK, et al. Gene set enrichment analysis: a knowledge-based approach for interpreting genome-wide expression profiles. *Proc Natl Acad Sci USA.* 2005;102(43):15545-15550.
18. Heinz S, Benner C, Spann N, et al. Simple combinations of lineage-determining transcription factors prime cis-regulatory elements required for macrophage and B cell identities. *Mol Cell.* 2010;38(4):576-589.
19. Kaya-Okur HS, Wu SJ, Codomo CA, et al. CUT&Tag for efficient epigenomic profiling of small samples and single cells. *Nat Commun.* 2019;10(1):1930.
20. Yashar WM, Kong G, VanCampen J, et al. GoPeaks: histone modification peak calling for CUT& Tag. *bioRxiv.* Preprint posted online 14 January 2022.
21. Hurlin PJ, Quéva C, Eisenman RN. Mnt, a novel Max-interacting protein is coexpressed with Myc in proliferating cells and mediates repression at Myc binding sites. *Genes Dev.* 1997;11(1):44-58.
22. Tyner JW, Yang WF, Bankhead A III, et al. Kinase pathway dependence in primary human leukemias determined by rapid inhibitor screening. *Cancer Res.* 2013;73(1):285-296.
23. Ianevski A, He L, Aittokallio T, Tang J. SynergyFinder: a web application for analyzing drug combination dose-response matrix data. *Bioinformatics.* 2017;33(15):2413-2415.
24. Bliss C. The toxicity of poisons applied jointly. *Ann Appl Biol.* 1939;26:585-615.
25. Rohrabaugh S, Kesarwani M, Kincaid Z, et al. Enhanced MAPK signaling is essential for CSF3R-induced leukemia. *Leukemia.* 2017;31(8):1770-1778.
26. Zhang H, Coblentz C, Watanabe-Smith K, et al. Gain-of-function mutations in granulocyte colony-stimulating factor receptor (CSF3R) reveal distinct mechanisms of CSF3R activation. *J Biol Chem.* 2018;293(19):7387-7396.
27. Zhang H, Reister Schultz A, Luty S, et al. Characterization of the leukemogenic potential of distal cytoplasmic CSF3R truncation and missense mutations. *Leukemia.* 2017;31(12):2752-2760.
28. Maxson JE, Luty SB, MacManiman JD, Abel ML, Druker BJ, Tyner JW. Ligand independence of the T618I mutation in the colony-stimulating factor 3 receptor (CSF3R) protein results from loss of O-linked glycosylation and increased receptor dimerization. *J Biol Chem.* 2014;289(9):5820-5827.
29. Tyner JW, Tognon CE, Bottomly D, et al. Functional genomic landscape of acute myeloid leukaemia. *Nature.* 2018;562(7728):526-531.
30. Cogswell JP, Cogswell PC, Kuehl WM, et al. Mechanism of c-myc regulation by c-Myb in different cell lineages. *Mol Cell Biol.* 1993;13(5):2858-2869.
31. Pacharne S, Dovey OM, Cooper JL, et al. SETBP1 overexpression acts in the place of class-defining mutations to drive FLT3-ITD-mutant AML. *Blood Adv.* 2021;5(9):2412-2425.
32. Amente S, Bertoni A, Morano A, Lania L, Avvedimento EV, Majello B. LSD1-mediated demethylation of histone H3 lysine 4 triggers Myc-induced transcription. *Oncogene.* 2010;29(25):3691-3702.
33. Nguyen N, Gudmundsson KO, Soltis AR, et al. Recruitment of MLL1 complex is essential for SETBP1 to induce myeloid transformation. *iScience.* 2021;25(1):103679.
34. Delgado MD, León J. Myc roles in hematopoiesis and leukemia. *Genes Cancer.* 2010;1(6):605-616.
35. Braun TP, Coblentz C, Curtiss BM, et al. Combined inhibition of JAK/STAT pathway and lysine-specific demethylase 1 as a therapeutic strategy in CSF3R/CEBPA mutant acute myeloid leukemia. *Proc Natl Acad Sci USA.* 2020;117(24):13670-13679.
36. Maiques-Diaz A, Spencer GJ, Lynch JT, et al. Enhancer activation by pharmacologic displacement of LSD1 from GFI1 induces differentiation in acute myeloid leukemia. *Cell Rep.* 2018;22(13):3641-3659.
37. Cusan M, Cai SF, Mohammad HP, et al. LSD1 inhibition exerts its antileukemic effect by recommissioning PU.1- and C/EBPα-dependent enhancers in AML. *Blood.* 2018;131(15):1730-1742.
38. Smith BM, VanCampen J, Kong GL, et al. PU.1 and MYC transcriptional network defines synergistic drug responses to KIT and LSD1 inhibition in acute myeloid leukemia. *bioRxiv.* Preprint posted online 5 October 2021.